POLITECNICO
MILANO 1863

DIPARTIMENTO DI MECCANICA

mecc

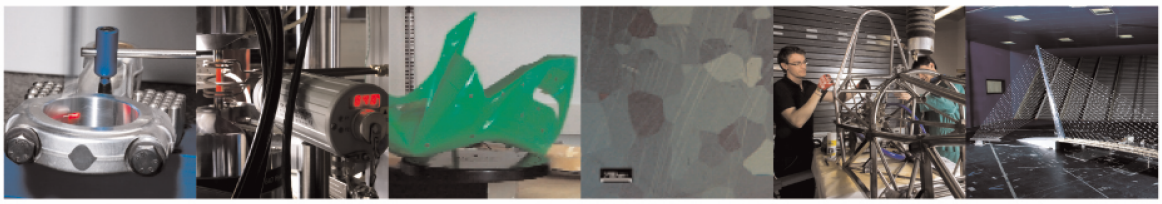

The influence of slicing parameters on the multi-material adhesion mechanisms of FDM printed parts: an exploratory study

Francesco Tamburrino, Serena Graziosi, Monica Bordegoni

This is an Accepted Manuscript of an article published by Taylor & Francis in Virtual and Physical Prototyping on 23 April 2019, available online:
http://www.tandfonline.com/10.1080/17452759.2019.1607758.

DIPARTIMENTO DI MECCANICA ■ POLITECNICO DI MILANO
via G. La Masa, 1 ■ 20156 Milano ■ EMAIL (PEC): pecmecc@cert.polimi.it
http://www.mecc.polimi.it
Rev. 0

The influence of slicing parameters on the multi-material adhesion mechanisms of FDM printed parts: an exploratory study

Francesco Tamburrino[a], Serena Graziosi[b] and Monica Bordegoni[b]

[a] Università di Pisa, Department of Civil and Industrial Engineering, Pisa, Italy;

[b] Politecnico di Milano, Department of Mechanical Engineering, Milano, Italy

ARTICLE HISTORY
Compiled March 20, 2021

ABSTRACT
The potentiality of the Fused Deposition Modeling (FDM) process for multi-material printing has been not yet thoroughly explored in the literature. That is a limitation considering the wide diffusion of dual extruders printers and the possibility of increasing the number of these extruders. An exploratory study, based on tensile tests and performed on double-material butt-joined bars, was thus conceived; the aim was to explore how the adhesion strength between 3 pairs of filaments (TPU-PLA, PLA-CPE, CPE-TPU) is influenced by the material printing order, the type of slicing pattern used for the layers at the interface, and the infill density of the layers below the interface. Results confirm the effectiveness of mechanical interlocking strategies in increasing the adhesion strength even when thermodynamic and diffusion mechanisms of adhesion are not robust enough. Besides, thermal aspects also demonstrated to play a relevant role in influencing the performance of the interface.

KEYWORDS
Multi-material printing; Multi-material adhesion; Fused Deposition Modeling (FDM); Slicing parameters; Design for Additive Manufacturing

1. Introduction

Fused Deposition Modeling (FDM) is one of the most commonly used Additive Manufacturing (AM) technologies (Turner, Strong, & Gold, 2014). It is reliable, can count on a wide range of commercially available thermoplastic polymers, and requires low-cost investments (Carneiro, Silva, & Gomes, 2015).

During the FDM process, a filament of thermoplastic polymer is loaded, then melted and extruded through a nozzle and deposited according to programmed patterns. This process is repeated layer by layer. When the filament is extruded onto a previous layer (usually in a semi-molten state), the surface of this layer re-melts forming a polymer bond with the layer on its top (Patterson, Bahumanyam, Katragadda, & Messimer, 2018). Process parameters such as printing temperatures, printing speed, build orientation, layer thickness, infill density and pattern can all have a significant impact on the mechanical properties, and on the quality of the manufactured parts (Carneiro et al., 2015; Chacón, Caminero, García-Plaza, & Núñez, 2017). Besides, this technology allows printing multiple materials (Gao et al., 2015; Vaezi, Chianrabutra,

CONTACT Serena Graziosi. Email: serena.graziosi@polimi.it

Mellor, & Yang, 2013), maximum two (i.e., by using two extruders), even if further attempts to extend this limit are described in the literature (Espalin, Ramirez, Medina, & Wicker, 2014; Mosaic, 2018).

The multi-material printing is nowadays of broad interest. It allows creating multi-material functionally graded parts, objects with enhanced performances, and 4D printing structures (Garland & Fadel, 2015; Loh, Pei, Harrison, & Monzón, 2018; Lumpe, Mueller, & Shea, 2019; Tibbits, 2014; Vaezi et al., 2013). Currently, the most used and reliable AM technology for multi-material printing is the material jetting (Gao et al., 2015), which can build multi-material and multi-colour structures (Bourell et al., 2017) through the use of multiple inkjet-heads. Hence, as already underlined in (Lopes, Silva, & Carneiro, 2018), most of the studies on multi-material printing are based on the material jetting technology, such as the interesting works of (Lumpe et al., 2019; Mueller, Courty, Spielhofer, Spolenak, & Shea, 2017), and only a few investigated the bonding mechanisms occurring in multi-material FDM objects (Yin, Lu, Fu, Huang, & Zheng, 2018). However, the polyjet technology is currently more expensive, regarding both apparatus and materials, than the FDM one (Ligon, Liska, Stampfl, Gurr, & Mülhaupt, 2017).

Hence, the primary focus of this paper is to provide insights into the understanding of the multi-material FDM printing process. The paper aims at assessing significance and effect of some specific slicing parameters (the top layer slicing pattern, the printing order of materials, and the infill density) on the adhesion strength between three pairs of commercial filaments. Experimental tests were run using the Ultimaker 3 machine with two extruders (Ultimaker, 2018d), and the Ultimaker Cura 3.1.0 software (Ultimaker, 2018e) for generating the printing instructions. As samples double-material butt-joined bars were printed to test the adhesion strength of the following three pairs of materials: PLA (Ultimaker, 2018b) and TPU (Ultimaker, 2018c), CPE (Ultimaker, 2018a) and TPU (Ultimaker, 2018c), CPE (Ultimaker, 2018a) and PLA (Ultimaker, 2018b).

The final target of this research is to extend the Design for Additive Manufacturing (DfAM) background knowledge on multi-material printing. This paper can be beneficial to designers who want to develop multi-material FDM objects (e.g., by combining materials with a different elastic modulus like TPU and PLA) without the need for glues, joints or assembly operations. Besides, results may be used by developers of slicing software to enrich their products with new features handling the multi-material printing process. A desktop FDM machine was intentionally used to reach the widest audience of makers.

The paper is structured as follows. A selection of studies focused on the influence of printing parameters on the characteristics of the FDM objects and theories explaining the adhesion mechanisms among materials is reviewed in Section 2. Section 3 details the experimental methodology with a focus on the specimens design and prototyping. In Section 4, results are discussed, highlighting the influence of the parameters analysed. While in Section 5, printing guidelines are derived. Finally, conclusions are provided in Section 6.

2. Background

2.1. The influence of process and toolpath parameters

The literature on Additive Manufacturing (AM) reports several interesting studies focused on exploring the parameters influencing the FDM printing process and thus the properties of the printed objects. For example, the work of Turner and Gold (2015) provides an interesting overview of such parameters. Among those, *toolpath* and *process parameters* are mentioned. The former are, e.g. the deposition width, the layer height, the gap among deposition lines, the build orientation and the raster pattern (Turner & Gold, 2015). Examples of the latter are the filament melting temperature, the temperature of the printing environment and the extruder feed rate (Turner & Gold, 2015).

The work of Chacón et al. (2017) analyses both *process* and *toolpath parameters*. They studied the influence of the build orientation (upright, on-edge and flat), layer thickness and feed rate on the mechanical behaviour of PLA samples through tensile and 3-point bending tests. Their study demonstrates that samples with on-edge and horizontal orientation have higher mechanical performance and ductility than samples with upright orientation. Moreover, in the case of upright samples, the tensile and flexural strengths increase when the layer thickness increases, while their ductility decreases when the layer thickness increases. The effect of feed rate on tensile and flexural strength is not significant for on-edge and flat build orientation, while in upright samples as the feed rate increases the mechanical strength decreases. For all the build orientations, instead, as the feed rate increases, the ductility decreases (Chacón et al., 2017). Zhang, Wang, Yu, and Deng (2017) studied the following parameters: temperature of the printing nozzle; temperature of the build plate and the printing environment; layer thickness; printing speed. They drew interesting conclusions such as: the reheating effect of a deposited raster on a cooler one is a phenomenon that occurs mainly in the layer thickness printing direction; the increasing of the layer thickness has a positive influence on the inter-layer bonding strength since it allows reducing the temperature gradient, the cooling rate and, thus, the internal stresses; a high printing speed determines a decrease in the overall cooling rate. Their study highlights the importance of temperature management in the FDM process and its effect on the inter-layer bonding and, thus, on the mechanical behaviour of the printed part (Zhang et al., 2017).

The thermal aspect is also discussed in G. Goh et al. (2019). The authors provide a review of the mechanical properties of polymeric materials manufactured using the FDM technology. In particular, they investigated the effects of printing parameters such as raster angle, infill, and specimen orientation on mechanical properties such as tensile, compressive, flexural properties. They highlight the importance of modelling temperature variation, which would allow predicting the mechanical properties resulting from selected printing parameters. However, they underline also that the fast heating and cooling nature of the process is hard to be predicted using conventional theories and models.

Both Eiliat and Urbanic (2018) and Wang, Xie, Weng, Senthil, and Wu (2016) investigated *toolpath parameters* (Turner & Gold, 2015); they analysed the influence of voids and discontinuities on the mechanical behaviour of FDM parts since the presence of such unwanted voids can lead to unexpected failures. Eiliat and Urbanic (2018) propose an infill methodology based on the optimisation of parameters such as bead height (i.e. layer height), bead width (i.e. line width) and raster angle, with

the aim of reducing the presence of voids inside the part. The method is applied and validated for different geometries such as convex shapes, solids with internal holes, components with multiple 2D extrusions and complex 3D shapes. The proposed infill methodology allows reducing the presence of voids up to 8% (Eiliat & Urbanic, 2018). In (Wang et al., 2016) the mechanism of interlaminar void formation is discussed, and a method, based on the addition of thermally expandable microspheres into the thermoplastic filament, is proposed. This method resulted in a reduction of the voids number and size, leading to improved adhesion between deposition lines and, thus, to a higher tensile strength (Wang et al., 2016). G. D. Goh, Yap, Agarwala, and Yeong (2019) also deepened the aspects related to the presence of voids for parts printed using the FDM technology. They show how for fibre-reinforced composites, the number and size of voids decrease, similarly to what happens thanks to the presence of thermally expandable microspheres, as described in (Wang et al., 2016).

The work of Fernandez-Vicente, Calle, Ferrandiz, and Conejero (2016) also focuses on *toolpath parameters*. Indeed, they explored the influence of infill pattern and density on the tensile strength of ABS samples. They demonstrated that the selected infill pattern (*rectilinear, honeycomb* and *line*), has not a high influence on the tensile strength. Otherwise, the percentage of infill density has the highest and most significant impact on the tensile strength of the samples. The samples manufactured by setting 100% infill, and both *rectilinear* or *honeycomb* infill patterns are characterised by values of tensile strength with a difference of less than 1% from raw ABS material. As "raw" material the authors mean samples produced using the same ABS filament of the 3D printed samples, but cut into pellets in a plastic shredder and injection-moulded (Fernandez-Vicente et al., 2016).

The influence of *process parameters* such as print temperature, print speed and cooling fan speed has been intensely investigated in (Jiang, Hu, et al., 2019; Jiang, Lou, & Hu, 2019; Jiang, Stringer, & Xu, 2018; Jiang, Stringer, Xu, & Zheng, 2018; Jiang, Stringer, Xu, & Zhong, 2018; Jiang, Xu, & Stringer, 2018). These studies explored the influence of these process parameters on support optimisation and, on the printable bridge length. In (Jiang, Stringer, & Xu, 2018; Jiang, Stringer, Xu, & Zhong, 2018) it is demonstrated how these factors have an impact on the strength and accuracy of the 3D printed part. In (Jiang, Lou, & Hu, 2019) the authors show how the above-described parameters also affect surface roughness and flexural properties. In (Jiang, Hu, et al., 2019) a method is developed which, through the process parameters optimisation, allows increasing the printable bridge length. All the works mentioned highlight how the connection status between each layer is influenced by process parameters such as print temperature, print speed, cooling fan speed, layer thickness. The connection status between the layers is of fundamental importance to get a good adhesion in extrusion-based processes.

In the literature, many more studies are available exploring the influence of FDM printing parameters such as the review of Popescu, Zapciu, Amza, Baciu, and Marinescu (2018) and Mohan, Senthil, Vinodh, and Jayanth (2017); there are also studies focused on guiding users in calibrating their machine to reduce the dimensional mismatch between the printed part and its 3D model, such as the work of Santana, Alves, and da Costa Sabino Netto (2017). However, as already underlined in Section 1, less effort has been spent on exploring their influence in multi-material parts. Nevertheless, some relevant studies were recently published. For example, in (Lopes et al., 2018) the interface zone between two different materials is explored considering both *toolpath* and *process parameters*. Besides, the role of the interface is analysed using the same filament for both extruders. This study underlines the importance of the chemical

affinity between the two materials and the relevance that the design of the interface plays in determining the performance of the adhesion. In (Yin et al., 2018) a theoretical model is developed and tested to evaluate the influence of process parameters, such as the temperature of the building stage, the nozzle temperature and the printing speed.

The research described in this paper is in line with the one of Lopes et al. (2018) and Yin et al. (2018), but it also has some distinguishing features. First, to experimentally evaluate the practical adhesion and the influence of the slicing variables, the ASTM D2095 - 96 standard test method (ASTM, 2015), conceived for the testing of adhesives, has been used. Second, samples were printed using a vertical orientation to intentionally exclude the influence of the building plate temperature on the adhesion strength, since the adhesion between the two materials occurs far away from the building plate (Yin et al. (2018)). Third, tests were conceived with the intent of deriving guidelines for users of dual-extrusion FDM machines. Such guidelines will be discussed in Section 5.

2.2. Main aspects involved in adhesion mechanisms

Multiple aspects influence the adhesion mechanisms among materials such as their macromolecular structure or the physical chemistry of their surfaces at the interface and their rheology (see (Schultz & Nardin, 1999)). The aim of this Section is not to minutely cover all the theories available but rather to discuss some of the main aspects involved in multi-material printing to justify the method used and the considerations derived from the experimental tests.

First, it is necessary to make a distinction between practical and fundamental adhesion. Practical adhesion is the phenomenon that will be investigated in this paper. It is related to the magnitude of mechanical force or energy to apply in order to produce a failure of an adhesive bond and it is assessed through mechanical tests. Fundamental adhesion, instead, is a phenomenon related to forces and mechanisms involved on the molecular scale when holding together a substrate with an adhesive. Thus, it can be considered as a *prerequisite* for the practical adhesion (da Silva, Öchsner, & Adams, 2011).

One of the theories related to the adhesion mechanisms is the mechanical theory, also known as mechanical keying or interlocking. This theory is mainly related to the characteristics of the surfaces of adhesive and substrate, as the presence of asperities, pores, cavities and roughness. In particular, the roughness influences the practical adhesion. As reported in (da Silva et al., 2011; Pizzi & Mittal, 1999), the voids created by the roughness at the interface between substrate and adhesive, if a brittle material is used as adhesive, act as the point of stress concentration, lowering the practical adhesion. Otherwise, in the case of ductile adhesives, the stress concentration, due to the roughness, can enhance the practical adhesion through local plastic deformations that increase the amount of energy dissipated during the failure (da Silva et al., 2011; Pizzi & Mittal, 1999).

However, other aspects are involved in the adhesion mechanisms (da Silva et al., 2011; Kinloch, 1980; Pizzi & Mittal, 1999). One of those are the forces, considered and described by the thermodynamic theory, which act between substrate and adhesive. In particular, surface energies and surface tensions, and their incidence on the contact angle between substrate and adhesive, are explored (the contact angle determines the wettability of a substrate). The essential idea of this theory is that the contact between

two materials is fundamental to establish interatomic and intermolecular forces at the interface between these two materials. The magnitude of the forces depends on the chemical nature of the surfaces of the substrate and the adhesive. Manufacturing process and geometric aspects, such as surface roughness, influence the effectiveness of the thermodynamic theory of adhesion. If the roughness value of the substrate is not high enough its effect on wettability is not significant. Otherwise, if the roughness is high, the wettability of the substrate is reduced, and it negatively affects the joint strength between the substrate and the adhesive (da Silva et al., 2011; Packham, 2003; Pizzi & Mittal, 1999).

Another theory proposed for adhesion mechanisms is the diffusion one, which is based on the assumption that the adhesion strength of a polymer to itself (*autohesion*) or, to another kind of polymer, is due to a mutual diffusion of macromolecules across the interface and, thus, relies on the dynamics of polymer chains in the interfacial region (Pizzi & Mittal, 1999). These dynamics are influenced by factors such as the temperature, the contact time between the polymers, their nature and their molecular weight. Diffusion phenomena can thus significantly contribute to the adhesion strength. Precisely, some conditions should be fulfilled in case the substrate and the adhesive are two different polymers. For example, the polymers need to be sufficiently soluble; adequate mobility should characterise their chains and, thus, they should not be highly cross-linked or crystalline; they need to be placed in contact at a temperature that is higher than the glass transition of the substrate (da Silva et al., 2011; Pizzi & Mittal, 1999).

Finally, it is worth highlighting that all the theories described in this section are valid, but each one is partial, cannot be considered universal and needs to be integrated with the others. Adhesion science is a multidisciplinary field, and this section is only aimed to provide an overall overview of this complex and articulated topic.

3. Materials and methods

The adhesion of the following three pairs of filaments was tested: PLA (Ultimaker, 2018b) and TPU (Ultimaker, 2018c), CPE (Ultimaker, 2018a) and TPU (Ultimaker, 2018c), CPE (Ultimaker, 2018a) and PLA (Ultimaker, 2018b). The following official Ultimaker materials were chosen: PLA Silver Metallic (extrusion temperature 205°C); CPE Blue (extrusion temperature 250°C); TPU 95A White (extrusion temperature 225°C). The PLA filament is brittle, the CPE is resilient, and the TPU 95A (from now on called only TPU) is semi-flexible.

As anticipated in Section 1, the dual-extrusion *Ultimaker 3* machine (Ultimaker, 2018d) (nozzle diameter 0.4 mm) and the Ultimaker Cura 3.1.0 software (Ultimaker, 2018e) were used. The specimens, for the tensile tests, are butt-joined bars (Figure 1) as defined in the standard test method ASTM D2095 - 96 (ASTM, 2015). The standard practice for the attachment fixtures, self-aligning, and testing procedure was followed, but the geometry and the dimensions of the sample have been modified to address some technological issues related to the manufacturing process of the samples. For example, a rectangular instead of a square cross-section (Figure 1) was used to increase the surface of adhesion of the sample and guarantee a good adhesion to the build plate during the printing process. Besides, any geometric feature that could have somehow influenced the mechanical interlocking between the two materials, and any adhesion promotion technique, such as plasma treatments (Hegemann, Brunner, & Oehr, 2003), were intentionally avoided. This choice was driven by the intent of focusing the study

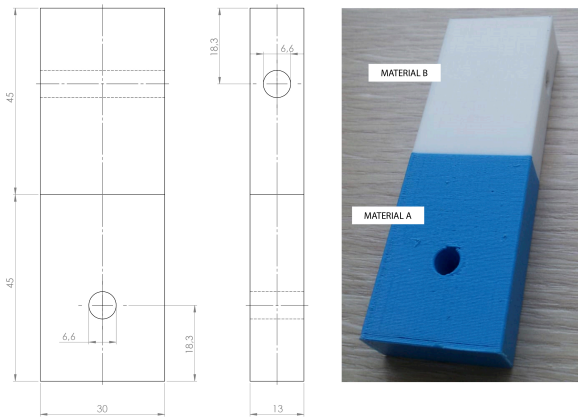

Figure 1. The geometry of the samples designed for tensile tests. An image of the printed sample is also provided: the material "A" is CPE (Ultimaker, 2018a) while the material "B" is TPU (Ultimaker, 2018c).

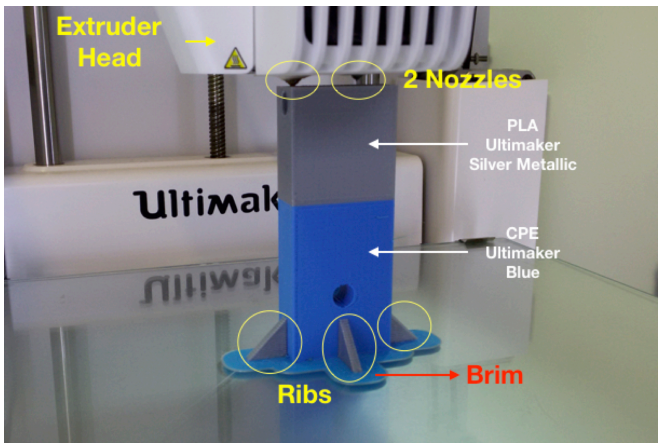

Figure 2. To guarantee a good adhesion of the sample to the build plate, four ribs and the Ultimaker Cura feature called "Brim" (the flat area at the basis of the sample), were used. This picture was taken during the final printing phases of one of the CPE-PLA samples. The two nozzles of the *Ultimaker 3* machine (Ultimaker, 2018d) are also shown.

only on the contribution of the slicing strategies and material printing order on the adhesion performance.

Each sample was printed separately (Figure 2) to guarantee that samples with equal printing parameters were built using the same printing path. Besides they were all printed with a layer thickness of 0.3 mm and a vertical orientation. To avoid the risk of warping of the bottom layers and the sample detaching from the build plate, 4 ribs and the so-called "brim" feature (available in the Ultimaker Cura software) were added. This solution was used to guarantee the stability of the specimen during the printing process (see Figure 2). They were removed before running the tensile tests.

Figures 3 and 4 clarify some aspects and terms that are central to this study. Each half of the sample (the height of each half is 45 mm, Figure 1) consists of 150 layers (Figure 3) since a layer thickness of 0.3 mm was selected. These 150 layers can be clustered as 3 bottom layers, 144 intermediate layers and 3 top layers. *Bottom* and *top layers* are, respectively, the first and the last layers printed (Figure 3), and they can be more than one. They have 100% density (see Figure 4b), and they contribute to getting a good external finishing (in the case of the *top layers*) and adhesion to

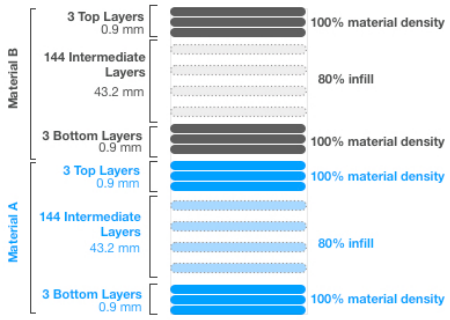

Figure 3. A graphical representation of the "0" configuration of the sample. Each half is built with 3 bottom layers, 144 intermediate layers, and 3 top layers. The "standard" interface consists of the last top layer of material "A" and the first bottom layer of material "B". In this configuration, the intermediate layers are printed using 80% infill while the top/bottom layers can have only 100% density.

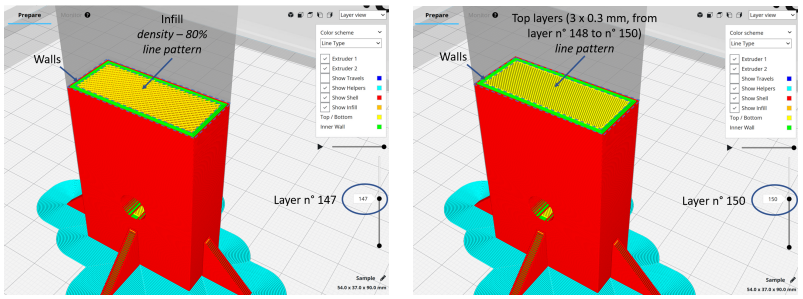

(a) (b)

Figure 4. Each layer of the sample is divided into two zones: the "walls" and the internal area called "infill". For each sample, walls were printed with 3 lines. The width of each line is set equal to the nozzle diameter (i.e., 0.4 mm). Layers from n°4 to n°147 are printed using 80% infill (4a); layers from n°148 to n°150 are the top ones of the bottom material (see Figure 3), and they have 100% density (4b). In the two images, the same type of slicing pattern (i.e., *Lines*) is used for the intermediate and top layers (further details will be provided in Figure 6).

the plate (in the case of the *bottom layers*). Actually, the adhesion to the plate is guaranteed by the first layer printed, which is part of the bottom layers. Indeed, as it will be explained later on in this Section, for this layer a different and lower print speed is usually selected. As shown in Figure 3, a "standard" interface consists of the last top layer of the first material and the first bottom layer of the second material. It is defined as "standard" since other types of interfaces were also tested, as it will be explained later on. The intermediate layers (from layer n°4 to layer n°147) can be printed using an infill below 100% (Figure 4a). That is usually done to save material and reduce the weight of the printed part. We used 80% infill for the "0" configuration of the sample.

In this study, the influence of the following *toolpath* variables (see Section 2.1), on the adhesion strength, was tested:

- materials printing order for each pair;
- type of pattern used for the top/bottom layers;
- infill density of the intermediate layers.

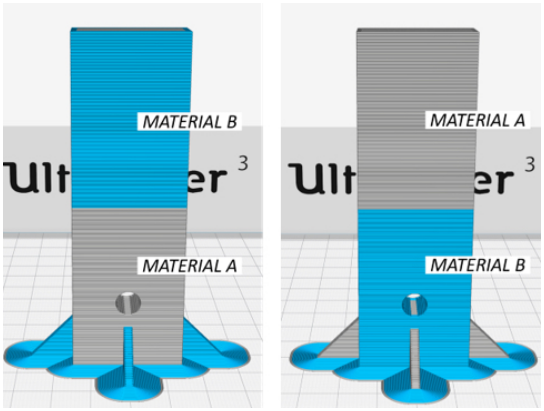

Figure 5. The meaning of the variable "materials printing order": for each pair, these two configurations were printed.

The influence of the material printing order was tested to check whether the object orientation on the build plate (Figure 5) could somehow influence the strength of the adhesion.

The top/bottom layers are the ones involved in the interface (Figure 3). The main settings that can be modified (in the Ultimaker Cura 3.1.0 version) are the type of pattern used for building the cross-section of these layers and the number of layers (as already explained the density of these layers is 100%, see also Figure 4b). The number of layers was fixed at 3 to focus the study on the influence of the type of pattern. The Ultimaker Cura 3.1.0 software (Ultimaker, 2018e) allowed using the following top/bottom patterns: *Lines* (Figure 6a); *Zig Zag* (Figure 6b); *Concentric* (Figure 6c). The *Lines* pattern is the default one and was used as the reference. The *Concentric* pattern was tested, but the adhesion strength was meagre (the samples broke once printed). Hence, results related to this pattern are not shown. That was already an initial demonstration of the importance of the slicing pattern when combining two materials. An additional pattern was tested together with the *Lines* and *Zig Zag* ones to simulate a mechanical interlocking (see Section 2.2). This pattern was created on purpose, starting from the *Lines* and using the Cura feature that allows specifying the extruder to be used for printing top/bottom layers (Figure 4a): the result is still a *Lines* pattern, but the top layers of the first material are printed using the other material, while the walls using the first. Figure 6d shows the approach used to create such *Mechanical interlocking* (this is the label used in this paper to indicate this pattern).

Finally, the influence of the infill density of the intermediate layers (see Figure 3) was tested for the following two reasons. First, it is a setting that has always to be decided before printing. Second, it was useful to investigate whether such "intermediate" layers could have any role in the adhesion strength. Figure 7 shows the effect of the infill variation of the intermediate layers on the printing path (Figure 7a), and the configurations created to test this variable (Figures 7b and 7c). For both configurations, layers were printed using the *Lines* pattern but varying the infill density of the intermediate layers of the first material printed (100%, 80% and 60% infill were tested). Besides, with the configuration shown in Figure 7c, the effect of the infill density of the intermediate layers, on the *Mechanical interlocking* pattern (Figure 6d), was also tested.

Concerning the printing speed variable, the default profiles available in the Ul-

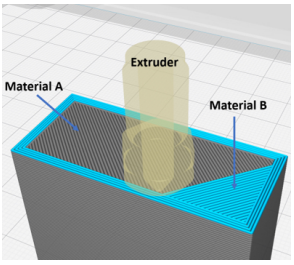

(a) *Lines* pattern (lines at 45°/135°)

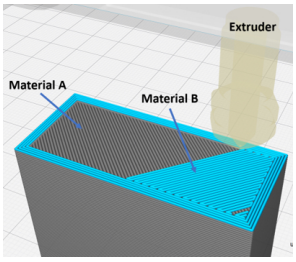

(b) *Zig-Zag* pattern (lines at 45°/135°)

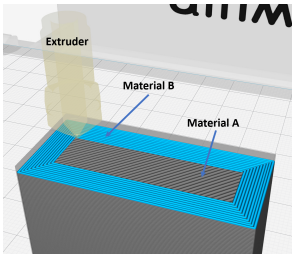

(c) *Concentric pattern*

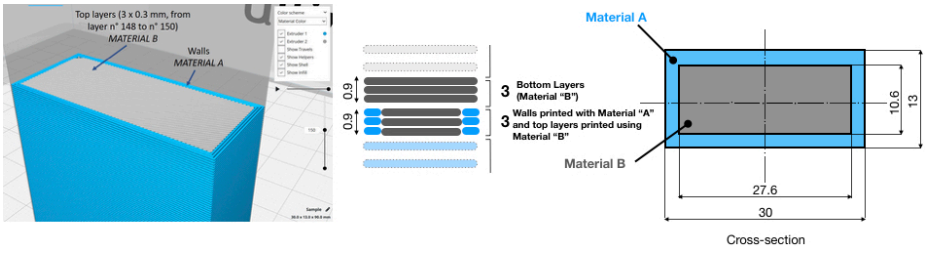

(d) *Mechanical interlocking* pattern obtained as a variation of the *Lines* pattern (6a) and by printing the material "A" top layers using the material "B" (see also Figure 3).

Figure 6. The three top/bottom slicing patterns (i.e., *Lines*, *Zig-Zag*, *Mechanical interlocking*) tested and the one excluded (i.e., the *Concentric*) since too weak. These images were generated using the ".STL" file of the sample (Figure 1) and the graphical outputs provided by the Ultimaker Cura software (Ultimaker, 2018e). "A" and "B" are used only to label the two materials. The three images are not correlated.

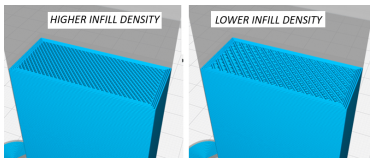

(a)

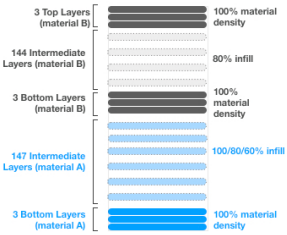

(b)

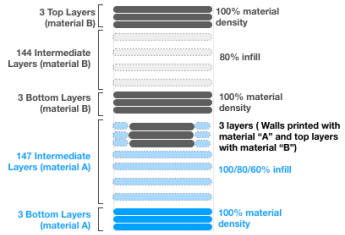

(c)

Figure 7. Figure 7a shows what occurs to the printing path when varying the infill density of the intermediate layers (see also Figure 3). Figures 7b and 7c show the two configurations of samples created to test this variable using 100%, 80%, and 60% infill. Figure 7c is the configuration used to test the infill density for the *Mechanical interlocking* pattern.

Table 1. Printing speed values used for printing the samples.

	Materials tested		
Speed (mm/s)	CPE Blue	PLA Silver Metallic	TPU 95A White
Print Speed	60	70	25
Wall Speed	45	50	25
Top/Bottom Speed	35	35	25
Travel Speed	250	250	300
Initial Layer Speed	20	20	18

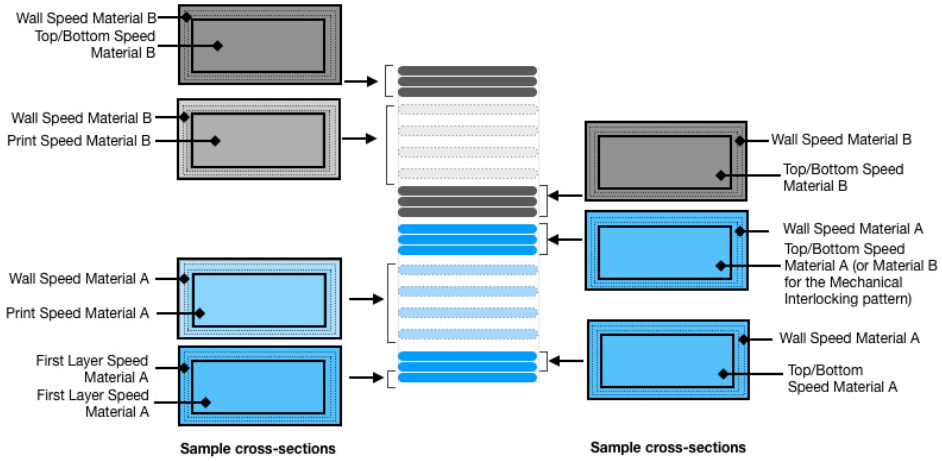

Figure 8. The image explains how, the printing speed values provided in Table 1, affect the different cross-sections of the samples.

timaker Cura 3.1.0 software were used. They are summarised in Table 1, while in Figure 8 the meaning of these values is explained. As Table 1 demonstrates, multiples are the speed variables that can be modified and, as already discussed in Section 2.1, the printing speed could influence the adhesion among layers, for example, by decreasing the cooling rate if the printing speed is increased (Zhang et al., 2017). Indeed, the increase of the printing speed leads to an increase of time needed to solidify the melted filament (Jiang, Hu, et al., 2019). However, in this study, the default values were intentionally considered, since the objective was to explore the influence of some of those slicing variables whose choice is entirely up to the user and his/her printing experience. It is evident that values, in particular, such as the *Top/Bottom Speed* and the *Wall Speed*, have contributed to determining the results that will be described in Section 4. For example, the work of Yin et al. (2018) demonstrates that changes in the printing speed alter the position in time of the peaks of temperature, but do not modify the pattern of the temperature at the interface. It is worth mentioning that in the study reported in Yin et al. (2018), a different sample was used and in particular, the interface of this sample is close to the building stage whose temperature instead significantly influences the bonding strength.

Specimens (Figure 1) were tested using the MTS Synergie 200 machine, using a 1kN load cell (Figure 9). Besides, a qualitative analysis through infrared thermography was carried out to observe the thermal gradients occurring at the interface between each pair of materials during the printing process. The *FLIR B335* thermal camera was used. From a thermal point of view, the FDM process is characterised by the heterogeneous distribution of the heat. This is mainly due to the intrinsic nature of the process and, in particular, to the reheating effect of the extruded filament on cooler layers, and

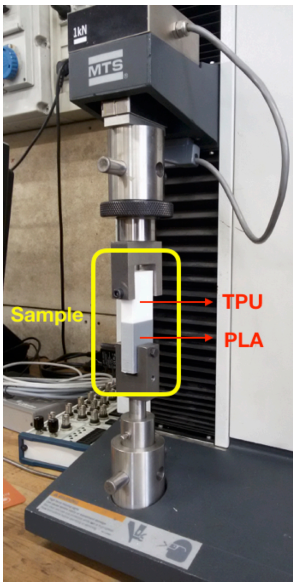

Figure 9. The tensile tests performed using the MTS Synergie 200 machine and a 1kN load cell. In this image, a PLA-TPU sample is also shown.

the path used by the extruder for the material deposition. That leads to the presence of welding zones between layers (Seppala & Migler, 2016; Wolszczak, Lygas, Paszko, & Wach, 2018; Zhang et al., 2017). Hence, the thermal gradients generated by this effect could vary with the printing setting (i.e., with the *process* and *toolpath parameters*) and could differently affect the adhesion mechanisms related to thermodynamic and diffusion (see Section 2.2). The analysis of the thermal gradients was used to derive further qualitative considerations about the results provided by the mechanical tests, and to understand better the influence of the different slicing strategies.

4. Results

The practical adhesion of three pairs of filaments (i.e., CPE and PLA, PLA and TPU, CPE and TPU) was tested printing 3 replicas for each pair and each parameter analysed. The influence of the 3 variables (i.e., material printing order, top/bottom infill pattern, infill density of the intermediate layers) presented in Section 3, are now discussed. As suggested by the standard test method used (ASTM, 2015), results are shown using the peak stress that was calculated dividing the breaking load by the area of the bonded surface.

4.1. The CPE-PLA pairs

For CPE-PLA pairs the following insights were retrieved:

- the adhesion strength is higher if the CPE is the first material printed (i.e., it is higher for the CPE-PLA pairs, see also Figure 10);
- the *Mechanical Interlocking* pattern (Figure 6d) increases the adhesion strength for both CPE-PLA and PLA-CPE pairs (Figure 10 and 11);

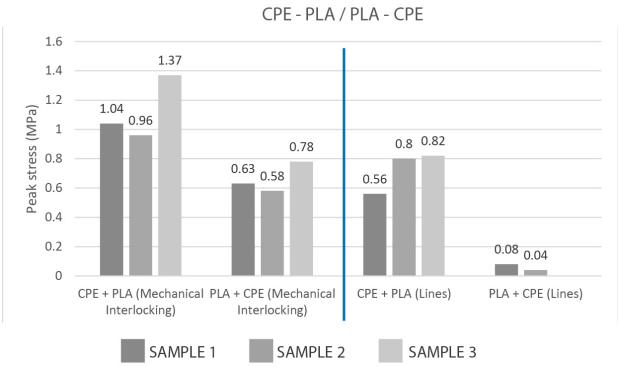

Figure 10. CPE-PLA and PLA-CPE pairs: the influence of the materials printing order on practical adhesion. The samples in which the CPE is the first material to be printed, have a higher adhesion strength. For the PLA-CPE pairs printed using the *Lines* pattern, only the results gathered by two samples are provided because the adhesion was so weak that the samples broke while setting up the machine gripping (indeed for this pair more than 3 replicas were printed).

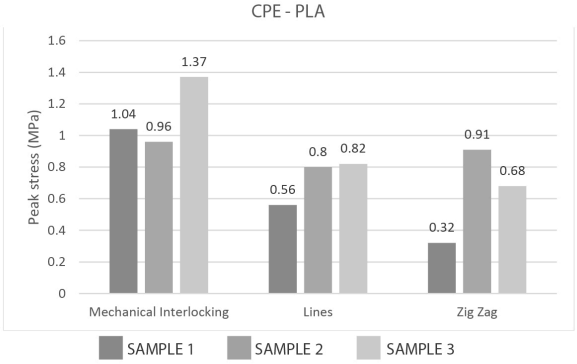

Figure 11. CPE-PLA pairs: the influence of the slicing pattern of the top/bottom layers on practical adhesion. The *Mechanical interlocking* pattern (Figure 6d) provides higher adhesion strengths than the *Lines* and the *Zig Zag* ones.

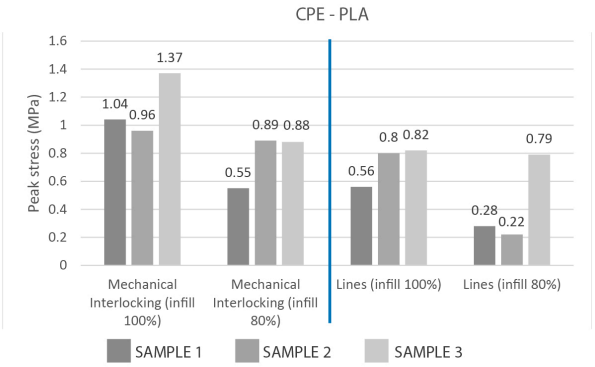

Figure 12. CPE-PLA pairs: the influence of infill density on practical adhesion (see also Figure 7). A decrease in the infill percentage leads to a decrease in the adhesion strength. This effect is valid both when the *Mechanical interlocking* and the *Lines* patterns are used for the top/bottom layers.

- the use of a lower infill density (100% and 80% infill were compared) has a negative impact on the adhesion strength for both CPE-PLA and PLA-CPE pairs (Figure 12).

Concerning the printing order, the following considerations are discussed. Despite CPE and PLA have different mechanical properties they can be considered as rigid materials. The printing temperature of the CPE is 250°C while for the PLA is 205°C. When printing CPE-PLA pairs, the difference in the printing temperature is 45°C. Hence, the thermal gradient is expected to gradually decreases considering that the last CPE layer will immediately start to cool down. Indeed, as discussed in Yin et al. (2018), the nozzle temperature affects the temperature peak values, but the profile of the temperature will, in any case, rapidly start to decrease. In the case of the PLA-CPE pairs since the last PLA layer will immediately start to cool down once printed, this thermal gradient should theoretically have the opposite behaviour. As already discussed in Section 2.1, the reduction of the thermal gradient has a positive effect on the adhesion strength. However, further tests should be performed to explore whether, in the case of rigid materials, it is always better to print first the material with the highest printing temperature.

Nevertheless, it is worth underlining that the considerations on the thermal gradients, occurring at the interface, are only based on the printing temperatures of the materials. These data are not sufficient to describe the thermal phenomena at the interface, as demonstrated in Yin et al. (2018). For a more in-depth understanding of the thermal aspects, quantitative and online measurements, through infrared thermography and/or thermocouples (Yin et al. (2018)) should be performed. Such an approach would allow having a point by point control of the temperature and the cooling rate during the printing process. As discussed in Section 2.2, the ideal condition for a good adhesion strength between two different polymers (at least for diffusion mechanisms of adhesion) would be a temperature for material B (i.e., the second material printed) higher than the glass transition of the material A (i.e., the first material printed), and a low cooling rate. These conditions, for all the three pairs of materials, and in the presence of a sufficient chemical affinity of the polymers, promote the mutual diffusion of their macromolecules across the interface.

For CPE-PLA pairs the *Mechanical interlocking* pattern (Figure 6d) promotes the adhesion mechanism known as *mechanical keying* or *interlocking* (da Silva et al., 2011; Kinloch, 1980; Pizzi & Mittal, 1999) thanks to the increase of the adhesion surface. However, the repeated switch between the two extruders, on the same layer and at the bonding area (the external walls are printed with the bottom material while the top layers enclosed in the walls are printed with the top material), affects the thermal gradient, and causes a faster cooling of the interface (see Figure 13). This characteristic could negatively affect the thermodynamic and diffusion mechanisms of adhesion. That is an interesting aspect to underline also looking at Figure 10 and considering what previously discussed concerning the printing order. Indeed, Figure 10 shows that PLA-CPE interfaces printed with the *Mechanical interlocking* pattern, performed similarly to the CPE-PLA pairs printed using the *Lines* pattern. Hence, in the case of PLA-CPA pairs, the *interlocking* effect is reduced by the thermal gradient at the interface of the two materials.

A higher cooling rate also occurs when lower percentages of infill density are used, due to the increase of the presence of voids within the sample (see Samples 2 and 3

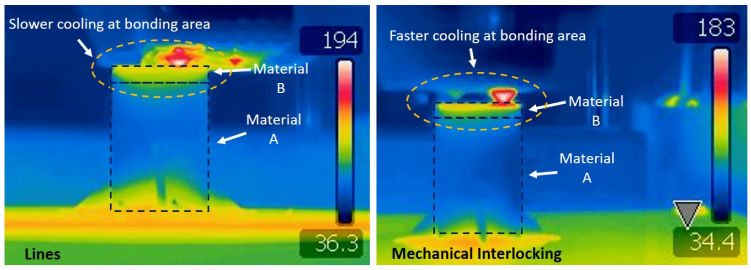

Figure 13. CPE-PLA pairs: influence of the *Lines* (on the left, see also Figure 6a) and of the *Mechanical Interlocking* (on the right, see also Figure 6d) patterns on thermal gradients at the bonding area during the printing process. This effect was observed for all the pairs of materials analysed.

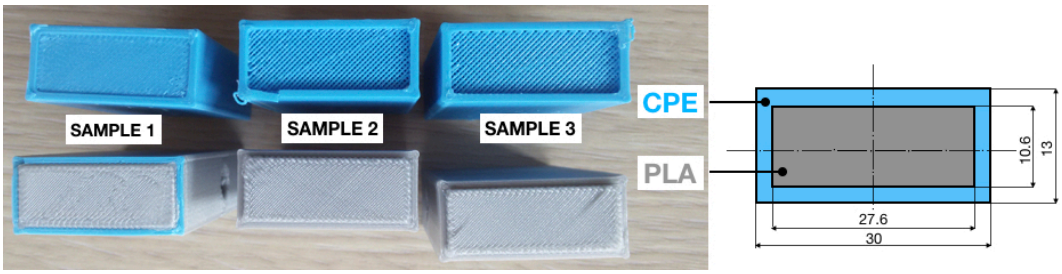

Figure 14. CPE-PLA pairs: examples of failures. These samples were printed using the *Mechanical Interlocking* pattern (CPE at the bottom and PLA at the top); in the case of sample 1 (infill 100%) the failure occurs because the CPE walls at the interface get broken while, in the case of samples 2 and 3 (infill 80%), the failure occurs because the PLA slips away causing the joint failure.

in Figure 14). In this case, there is also a reduction of the adhesion surface. This fact decreases the adhesion strength at the interface of the two materials (see Figure 12). The failures, shown in Figure 14, also demonstrate what previously underlined for the *Mechanical Interlocking* pattern, concerning thermodynamic and diffusion mechanisms of adhesion, since the two materials perfectly detach at the interface.

4.2. The PLA-TPU pairs

For PLA-TPU pairs the following observations were derived:

- the adhesion strength decreases if the TPU is the first material to be printed in particular with the *Mechanical interlocking* pattern (Figure 15);
- the *Mechanical interlocking* strategy increases the adhesion strength of PLA-TPU pairs (Figure 16);
- the use of a lower percentage of infill density (100% and 60% infill were compared) has a negative impact on the adhesion strength (Figure 17).

Regarding the material printing order (Figure 15), during the printing process the presence of a flexible and deformable material, at the bottom, could provide an unstable and not stiff base while printing. That effect is relevant especially when repeated changes of the extruder head have to be performed as in case of the *Mechanical Interlocking* pattern. In this case, it is preferred to have a stiff material at the bottom.

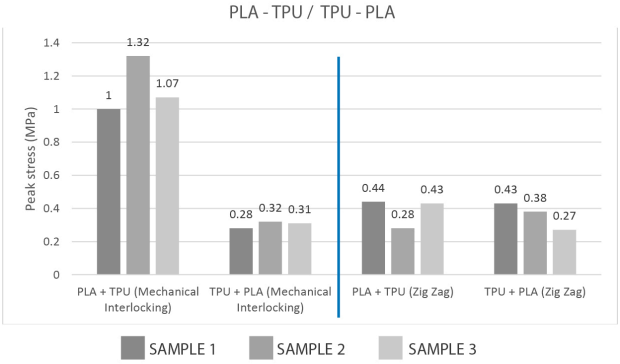

Figure 15. PLA-TPU and TPU-PLA pairs: influence of the materials printing order on practical adhesion. This effect is significant when the *Mechanical interlocking* pattern is used for the top layers.

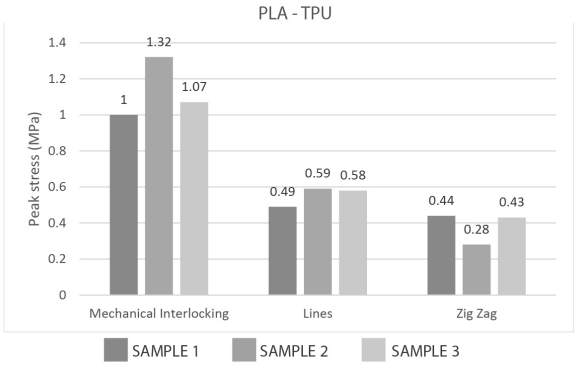

Figure 16. PLA-TPU pairs: influence of the slicing patterns on practical adhesion. The *Mechanical Interlocking* pattern provides higher adhesion strength compared to the *Lines* and the *Zig Zag* patterns.

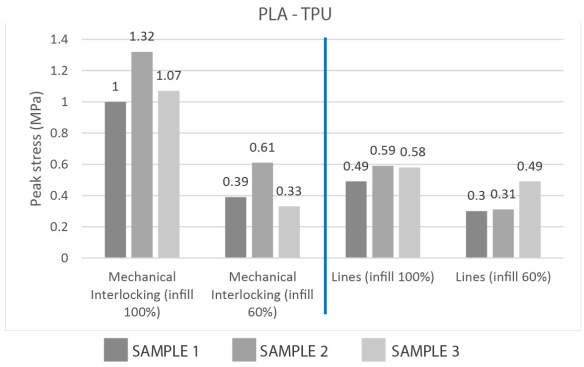

Figure 17. PLA-TPU pairs: influence of infill density on practical adhesion. A reduction of the infill density of the intermediate layers (see also Figure 7) leads to a decrease of the adhesion strength.

The difference in the printing temperature is now lower (i.e., 20°C) than the one of CPE and PLA (the TPU is printed at 225°C). Even if the material with the lowest printing temperature (i.e., the PLA which is extruded at 205°C) is printed as the first, the adhesion strength for the PLA-TPU interfaces, printed using the *Mechanical Interlocking* pattern, increases. Hence, the thermal aspect seems to be less significant than the side effects generated by the selected printing pattern. The influence of the printing order is, instead, less significant in the case of the *Zig-Zag* pattern (Figure 15).

The choice to use a different percentage of infill density for the intermediate layers (60%), lower than the density used for the CPE-PLA pairs (80%), was made for the following reason. In the presence of a semi-flexible material (TPU), a lower infill for the intermediate layers of the PLA part (printed as the first) could increase the energy dissipated viscoelastically or plastically around the crack tip and in the bulk of the semi-flexible material during the failure, improving the adhesion strength (see (da Silva et al., 2011; Kinloch, 1980; Pizzi & Mittal, 1999)). However, the results (Figure 17) do not show such an improvement. It is possible that local viscoelastic and plastic deformations are not so significant. Besides, the increase of the layer porosity (infill density 60% instead of 100%) decreases the overall adhesion surface at the interface, lowering the practical adhesion and, stimulates the presence of a thermal gradient between the two materials especially when the *Mechanical Interlocking* pattern is used (see also Figure 13).

4.3. The CPE-TPU pairs

For CPE-TPU pairs the following observations were derived:

- the adhesion strength decreases if the TPU is the first material to be printed when the *Mechanical Interlocking pattern* is used (Figure 18);
- the *Mechanical interlocking* strategy does not lead to a significantly higher adhesion strength (Figure 19);
- the use of a lower percentage of infill density (100% and 60% infill were tested) has a negative impact on the adhesion strength when the *Mechanical interlocking strategy is applied* (Figure 20).

The main difference with the previous pairs (i.e. PLA-TPU and CPE-PLA) is that the *Mechanical interlocking* strategy does not provide advantages in term of adhesion strength. Hence, for CPE-TPU pairs the type of pattern used does not significantly affect the adhesion strength (see Figure 19). That might mean that the compatibility between CPE and TPU due to thermodynamic and diffusion mechanisms of adhesion (see Section 2.2) is already robust enough, and its effect is thus not less significant than the mechanical interlocking. This fact is also demonstrated by the type of failures obtained (Figure 21).

The printing order was investigated only for the *Mechanical interlocking* pattern and results, similar to PLA-TPU pairs, were obtained. However, it is also worth highlighting that the CPE-TPU pairs are characterised by the best printing condition since not only the "rigid" material (i.e., the CPE) is the first to be printed, but it is also the material having the highest printing temperature (i.e., 250°C instead of 225°C for the

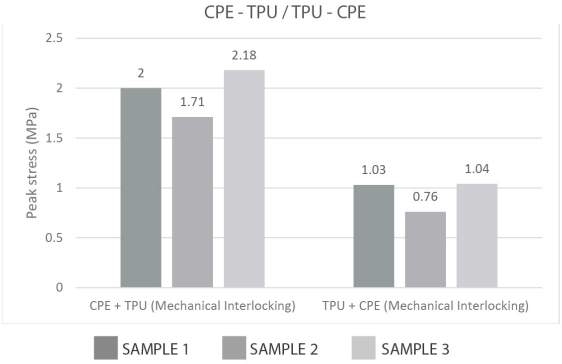

Figure 18. CPE-TPU and TPU-CPE pairs: influence of the materials printing order on practical adhesion. This effect was tested for the *Mechanical interlocking* pattern. The printing of the TPU as the first material provides a reduction of the adhesion strength.

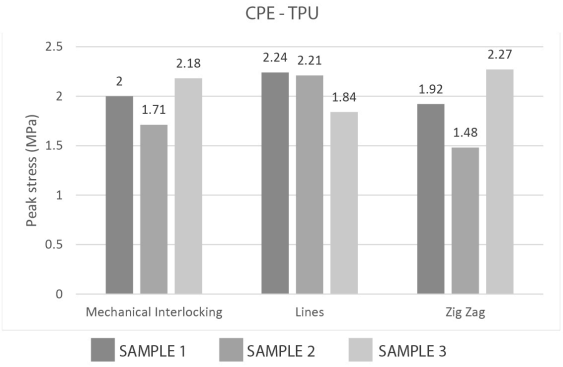

Figure 19. CPE-TPU pairs: influence of the slicing patterns on the practical adhesion. The type of slicing pattern used (i.e., *Mechanical interlocking*, *Lines* and *Zig Zag*) does not significantly influence the adhesion strength.

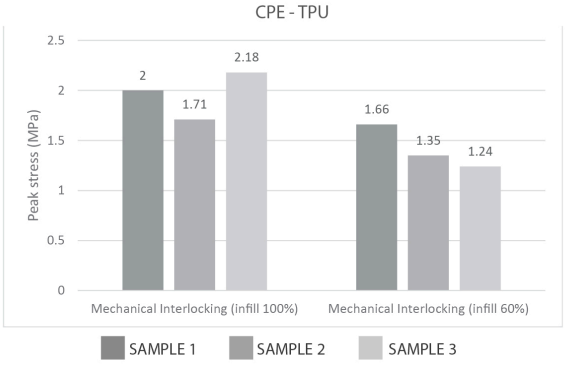

Figure 20. CPE-TPU pairs: the influence of the infill density on practical adhesion. The results show that a decrease of the infill density for the intermediate layers (Figure 7) leads to a decrease of the adhesion strength.

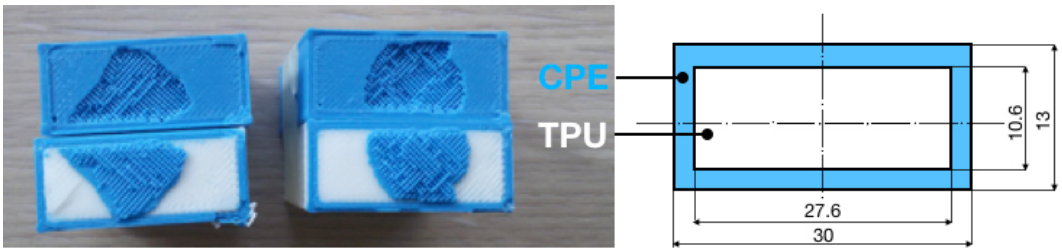

Figure 21. Examples of failures for the CPE-TPU pairs. The samples refer to the *Mechanical Interlocking* pattern (CPE at the bottom and TPU at the top). The CPE and the TPU filaments have a good degree of compatibility: after the failure of the joint, the materials at the interface are still partially joined.

TPU) (see Section 4.1). However, as already underlined, these data are not sufficient to describe the influence of the thermal aspects on the adhesion strength.

Finally, the results obtained concerning the infill density are aligned to what discussed in Section 4.1 and 4.2 for the other pairs in particular when the *Mechanical interlocking* strategy is selected.

5. Deriving printing guidelines

Given the above observations, to increase the adhesion strength between two materials, the following guidelines can be derived:

- when a stiff material and a semi-flexible or flexible one are butt-joined, the stiff material should be placed at the bottom (i.e., it should be printed as the first material) when mechanical interlocking effects, obtained as described in this study, are used to increase the adhesion strength of the interface;

- when thermodynamic and diffusion mechanisms of adhesion occurring between two materials are not robust enough (e.g., as in the case of CPE-PLA and PLA-TPU pairs) the *Mechanical interlocking* pattern could represent a valid approach to increase the adhesion strength;

- when two materials are butt-joined, a higher infill density should be set for the intermediate layers below the interface to increase the adhesion strength in particular when the *Mechanical interlocking* pattern, as designed in Figure 6d, is used.

The consideration related to the *Mechanical interlocking* pattern is in line with the results discussed in the work of Ribeiro, Carneiro, and da Silva (2018). Indeed, in that paper, it is demonstrated how, for pairs of materials characterised by low compatibility such as PLA and TPU, the creation of mechanical interfaces has a positive effect on the tensile strength of the samples. However, in the paper of Ribeiro et al. (2018), such interface is created in a CAD environment while in our case it is designed through the slicing software. That aspect also demonstrates that the slicing software is not only useful for generating printing instructions, but it represents a further design tool. Besides, in agreement with what discussed in Ribeiro et al. (2018) concerning the relevance of the chemical affinity between the pairs of materials on the adhesion strength, Figure 22 is provided. As the figure shows the best results in terms of adhesion

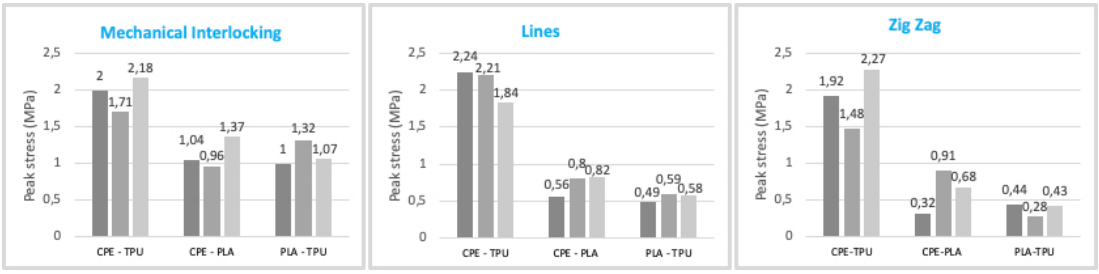

Figure 22. A comparison between the adhesion strengths and the slicing patterns used. The CPE-TPU pairs are the ones reaching the highest values.

strength are always obtained using the CPE-TPU pairs while the worst with the PLA-TPU pairs. Hence, this figure underlines once more that multiple aspects (e.g., thermal, mechanical, chemical) influence the adhesion strength between pairs of materials. It is also worth underlining that these considerations were derived without exploring the influence of the different printing speeds used (see Section 3). In addition, these considerations are based on a mechanical interlocking effect obtained as represented in Figure 6d. What represented in that figure is only one example of dimensioning of the interface. Further tests could be performed to explore how to properly design it (e.g., the optimal dimension of the walls thickness with respect to the internal area). Concerning the infill density of the intermediate layers, similar behaviours were registered especially when the *Mechanical interlocking* strategy is used (see Figures 12, 17 and 20). However, additional experiments are needed to demonstrate not only the persistence of this phenomenon for all the type of pattern selected for the interface but particularly to quantify it.

To conclude, it is also worth pointing out that the results presented in this section show significant deviations (considering the three specimens tested for each type of sample). These deviations are mainly due to thermal issues since the 3D printer used is not equipped with a closed and heated chamber. Indeed, the default configuration was intentionally not modified. The internal temperature of the chamber, during the additive process, was not controlled and this aspect, as discussed in Section 2.2, can affect the thermodynamic and diffusion mechanisms of adhesion (da Silva et al., 2011; Kinloch, 1980; Pizzi & Mittal, 1999). By using a 3D printer with a closed and heated chamber, such deviation should significantly decrease while also the thermal phenomena involved could significantly change, leading to different adhesion strengths.

6. Conclusions

The possibility to combine multiple materials during the printing process is an opportunity of high design relevance: the controlled and local combination of materials characterised by different mechanical behaviours allows extending Design for Additive Manufacturing (DfAM) opportunities. For example, 4D printing structures and the development of functionally graded parts are two research topics that can significantly benefit from this possibility. However, how to properly join materials having, for example, different mechanical behaviour or a low chemical affinity, is something that still needs further research efforts. Multiple printing aspects influence the adhesion among such materials, as demonstrated by the mechanical, thermodynamic and diffusion theories discussed in the literature (da Silva et al., 2011; Kinloch, 1980; Pizzi &

Mittal, 1999). However, while several studies are available concerning multi-material printing based on the material jetting technology, fewer research efforts have been put on investigating the multi-material FDM printing process.

In order to contribute to expanding the knowledge on this topic, this paper describes an exploratory study conceived to start exploring the influence of some slicing parameters on the adhesion strength between pairs of filaments. The following aspects were examined: the printing order of the materials; the slicing patterns used for printing the top/bottom layers; the infill density used to print the intermediate layers, i.e., the layers between the bottom and the top layers of each material. Three pairs of materials were tested using the Ultimaker 3 machine (Ultimaker, 2018d): PLA-TPU, CPE-TPU, CPE-PLA. Results demonstrate that the printing order of the material influences the adhesion strength (i.e., the stiff material should be the first to be printed) when mechanical interlocking effects, obtained as described in this paper, are used to increase the adhesion strength. These interlocking strategies are successful also when thermodynamic and diffusion mechanisms of adhesion are not robust enough. Also, given a specific pair of materials, the increase of the infill density of the intermediate layers leads to an increase of the adhesion strength especially when mechanical interlocking effects are applied.

Together with the results previously mentioned, this exploratory study also demonstrates the variability of the (thermal, mechanical, chemical) effects influencing the adhesion strength. Hence, further investigations are needed to identify better the correlation existing among these effects. For example, further studies are needed to more deeply explore the influence of the printing order of materials through a quantitative analysis of the thermal gradients occurring during the dual-extrusion printing process. Indeed, thermal aspects play a relevant role in influencing adhesion mechanisms. Besides, the influence of the printing speed could also be a further aspect to explore. Finally, this study also demonstrates once more, how much the slicing process is useful not only for generating printing instructions but also for designing the behaviour of the printed object.

Disclosure statement

No potential conflict of interest was reported by the authors.

Notes on contributor(s)

Francesco Tamburrino is Postdoctoral researcher at the Department of Civil and Industrial Engineering of Università di Pisa. His research activities are mainly focused on industrial design, materials science and technology, dental materials, cellular materials and Additive Manufacturing technologies.

Serena Graziosi is an Associate Professor in the Department of Mechanical Engineering of Politecnico di Milano. Her research activities are related to design methods, tools and processes for the industrial engineering and the development of new products/services; they involve all those technologies that can enhance the development process of new products/services, including, Virtual/Augmented Reality and Rapid Prototyping/Additive Manufacturing technologies.

Monica Bordegoni is Full Professor in the Department of Mechanical Engineering of Politecnico di Milano. Her research activities include Virtual and Physical Prototyping,

Multisensory systems, Olfactory Displays, Design for Additive Manufacturing.

References

ASTM. (2015). *Astm d2095 - 96, standard test method for tensile strength of adhesives by means of bar and rod specimens.*

Bourell, D., Kruth, J. P., Leu, M., Levy, G., Rosen, D., Beese, A. M., & Clare, A. (2017). Materials for additive manufacturing. *CIRP Annals*, *66*(2), 659 - 681. Retrieved from http://www.sciencedirect.com/science/article/pii/S0007850617301488

Carneiro, O., Silva, A., & Gomes, R. (2015). Fused deposition modeling with polypropylene. *Materials & Design*, *83*, 768–776.

Chacón, J., Caminero, M., García-Plaza, E., & Núñez, P. (2017). Additive manufacturing of pla structures using fused deposition modelling: effect of process parameters on mechanical properties and their optimal selection. *Materials & Design*, *124*, 143–157.

da Silva, L. F., Öchsner, A., & Adams, R. D. (2011). *Handbook of adhesion technology.* Springer: Heidelberg.

Eiliat, H., & Urbanic, R. J. (2018). Minimizing voids for a material extrusion-based process. *Rapid Prototyping Journal*, *24*(2), 485–500.

Espalin, D., Ramirez, J. A., Medina, F., & Wicker, R. (2014). Multi-material, multi-technology fdm: exploring build process variations. *Rapid Prototyping Journal*, *20*(3), 236-244. Retrieved from https://doi.org/10.1108/RPJ-12-2012-0112

Fernandez-Vicente, M., Calle, W., Ferrandiz, S., & Conejero, A. (2016). Effect of infill parameters on tensile mechanical behavior in desktop 3d printing. *3D printing and additive manufacturing*, *3*(3), 183–192.

Gao, W., Zhang, Y., Ramanujan, D., Ramani, K., Chen, Y., Williams, C. B., ... Zavattieri, P. D. (2015). The status, challenges, and future of additive manufacturing in engineering. *Computer-Aided Design*, *69*, 65 - 89. Retrieved from http://www.sciencedirect.com/science/article/pii/S0010448515000469

Garland, A., & Fadel, G. (2015, Oct). Design and manufacturing functionally gradient material objects with an off the shelf three-dimensional printer: Challenges and solutions. *Journal of Mechanical Design*, *137*(11), 111407. Retrieved from http://dx.doi.org/10.1115/1.4031097

Goh, G., Yap, Y., Tan, H., Sing, S., Goh, G., & Yeong, W. (2019). Process–structure–properties in polymer additive manufacturing via material extrusion: A review. *Critical Reviews in Solid State and Materials Sciences*, 1–21.

Goh, G. D., Yap, Y. L., Agarwala, S., & Yeong, W. Y. (2019). Recent progress in additive manufacturing of fiber reinforced polymer composite. *Advanced Materials Technologies*, *4*(1), 1800271.

Hegemann, D., Brunner, H., & Oehr, C. (2003). Plasma treatment of polymers for surface and adhesion improvement. *Nuclear instruments and methods in physics research section B: Beam interactions with materials and atoms*, *208*, 281–286.

Jiang, J., Hu, G., Li, X., Xu, X., Zheng, P., & Stringer, J. (2019). Analysis and prediction of printable bridge length in fused deposition modelling based on back propagation neural network. *Virtual and Physical Prototyping*, 1–14.

Jiang, J., Lou, J., & Hu, G. (2019). Effect of support on printed properties in fused deposition modelling processes. *Virtual and Physical Prototyping*, 1–8.

Jiang, J., Stringer, J., & Xu, X. (2018). Support optimization for flat features via path planning in additive manufacturing. *3D Printing and Additive Manufacturing*.

Jiang, J., Stringer, J., Xu, X., & Zheng, P. (2018). A benchmarking part for evaluating and comparing support structures of additive manufacturing.

Jiang, J., Stringer, J., Xu, X., & Zhong, R. Y. (2018). Investigation of printable threshold overhang angle in extrusion-based additive manufacturing for reducing support waste. *International Journal of Computer Integrated Manufacturing*, *31*(10), 961–969.

Jiang, J., Xu, X., & Stringer, J. (2018). Support structures for additive manufacturing: A review. *Journal of Manufacturing and Materials Processing*, *2*(4), 64.

Kinloch, A. (1980). The science of adhesion. *Journal of materials science*, *15*(9), 2141–2166.

Ligon, S. C., Liska, R., Stampfl, J., Gurr, M., & Mülhaupt, R. (2017). Polymers for 3d printing and customized additive manufacturing. *Chemical Reviews*.

Loh, G. H., Pei, E., Harrison, D., & Monzón, M. D. (2018). An overview of functionally graded additive manufacturing. *Additive Manufacturing*, *23*, 34 - 44. Retrieved from http://www.sciencedirect.com/science/article/pii/S221486041730564X

Lopes, L., Silva, A., & Carneiro, O. (2018). Multi-material 3d printing: the relevance of materials affinity on the boundary interface performance. *Additive Manufacturing*, *23*, 45-52. Retrieved from http://www.sciencedirect.com/science/article/pii/S2214860418301544

Lumpe, T. S., Mueller, J., & Shea, K. (2019). Tensile properties of multi-material interfaces in 3d printed parts. *Materials & Design*, *162*, 1 - 9. Retrieved from http://www.sciencedirect.com/science/article/pii/S0264127518308311

Mohan, N., Senthil, P., Vinodh, S., & Jayanth, N. (2017, Jan). A review on composite materials and process parameters optimisation for the fused deposition modelling process. *Virtual and Physical Prototyping*, *12*(1), 47–59. Retrieved from http://dx.doi.org/10.1080/17452759.2016.1274490

Mosaic. (2018). *Introducing palette 2.* Retrieved 31 October 2018, from https://www.mosaicmfg.com

Mueller, J., Courty, D., Spielhofer, M., Spolenak, R., & Shea, K. (2017). Mechanical properties of interfaces in inkjet 3d printed single- and multi-material parts. *3D Printing and Additive Manufacturing*, *4*(4), 193-199. Retrieved from https://doi.org/10.1089/3dp.2017.0038

Packham, D. (2003). Surface energy, surface topography and adhesion. *International Journal of Adhesion and Adhesives*, *23*(6), 437 - 448. Retrieved from http://www.sciencedirect.com/science/article/pii/S014374960300068X

Patterson, A. E., Bahumanyam, P., Katragadda, R., & Messimer, S. L. (2018). Automated assembly of discrete parts using fused deposition modeling. *Rapid Prototyping Journal*(just-accepted), 00–00.

Pizzi, A., & Mittal, K. (1999). *Adhesion promotion techniques.* Marcel Dekker, New York.

Popescu, D., Zapciu, A., Amza, C., Baciu, F., & Marinescu, R. (2018). Fdm process parameters influence over the mechanical properties of polymer specimens: A review. *Polymer Testing*, *69*, 157 - 166. Retrieved from http://www.sciencedirect.com/science/article/pii/S0142941818306093

Ribeiro, M., Carneiro, O. S., & da Silva, A. F. (2018). Interface geometries in 3d multi-material prints by fused filament fabrication. *Rapid Prototyping Journal*. Retrieved from https://doi.org/10.1108/RPJ-05-2017-0107

Santana, L., Alves, J. L., & da Costa Sabino Netto, A. (2017). A study of parametric calibration for low cost 3d printing: Seeking improvement in dimensional quality. *Materials & Design*, *135*, 159 - 172. Retrieved from http://www.sciencedirect.com/science/article/pii/S0264127517308523

Schultz, J., & Nardin, M. (1999). Theories and mechanisms of adhesion. *Materials Engineering -New York-*, *14*, 1–26.

Seppala, J. E., & Migler, K. D. (2016). Infrared thermography of welding zones produced by polymer extrusion additive manufacturing. *Additive manufacturing*, *12*, 71–76.

Tibbits, S. (2014, Jan). 4d printing: Multi-material shape change. *Architectural Design*, *84*(1), 116–121. Retrieved from http://dx.doi.org/10.1002/ad.1710

Turner, B. N., & Gold, S. A. (2015). A review of melt extrusion additive manufacturing processes: Ii. materials, dimensional accuracy, and surface roughness. *Rapid Prototyping Journal*, *21*(3), 250-261. Retrieved from https://doi.org/10.1108/RPJ-02-2013-0017

Turner, B. N., Strong, R., & Gold, S. A. (2014). A review of melt extrusion additive manufacturing processes: I. process design and modeling. *Rapid Prototyping Journal*, *20*(3),

192-204. Retrieved from https://doi.org/10.1108/RPJ-01-2013-0012

Ultimaker. (2018a). *Technical data sheet - ultimaker cpe.* Retrieved August 22 2018, from https://ultimaker.com/en/resources/49914-cpe

Ultimaker. (2018b). *Technical data sheet - ultimaker pla.* Retrieved August 22 2018, from https://ultimaker.com/en/resources/49911-pla

Ultimaker. (2018c). *Technical data sheet - ultimaker tpu.* Retrieved August 22 2018, from https://ultimaker.com/en/resources/49917-tpu-95a

Ultimaker. (2018d). *Ultimaker 3.* Retrieved August 3 2018, from https://ultimaker.com/en/products/ultimaker-3

Ultimaker. (2018e). *Ultimaker cura software.* Retrieved August 3 2018, from https://ultimaker.com/en/products/ultimaker-cura-software

Vaezi, M., Chianrabutra, S., Mellor, B., & Yang, S. (2013, Mar). Multiple material additive manufacturing – part 1: a review. *Virtual and Physical Prototyping*, *8*(1), 19–50. Retrieved from http://dx.doi.org/10.1080/17452759.2013.778175

Wang, J., Xie, H., Weng, Z., Senthil, T., & Wu, L. (2016). A novel approach to improve mechanical properties of parts fabricated by fused deposition modeling. *Materials & Design*, *105*, 152–159.

Wolszczak, P., Lygas, K., Paszko, M., & Wach, R. A. (2018, Apr). Heat distribution in material during fused deposition modelling. *Rapid Prototyping Journal*, *24*(3), 615–622. Retrieved from http://dx.doi.org/10.1108/RPJ-04-2017-0062

Yin, J., Lu, C., Fu, J., Huang, Y., & Zheng, Y. (2018). Interfacial bonding during multi-material fused deposition modeling (fdm) process due to inter-molecular diffusion. *Materials & Design*, *150*, 104 - 112. Retrieved from http://www.sciencedirect.com/science/article/pii/S0264127518302995

Zhang, J., Wang, X. Z., Yu, W. W., & Deng, Y. H. (2017). Numerical investigation of the influence of process conditions on the temperature variation in fused deposition modeling. *Materials & Design*, *130*, 59–68.